A BP Method for Track-Before-Detect: Supporting Derivations and Results

Mingchao Liang, Thomas Kropfreiter, and Florian Meyer

This manuscript provides derivations and further simulation results for the letter, "Belief Propagation for Track-Before-Detect" by the same authors [1].

1 Approximate Computation of BP Message $\kappa_{n,j}^{(\ell)}(\mathbf{y}_n)$

In this section, we derive the expression of the mean and covariance of message $\kappa_{n,j}^{(\ell)}(\mathbf{y}_n;\mathbf{z}_j)$, i.e., $\boldsymbol{\mu}_{\kappa,j}^{(\ell)}(\mathbf{y}_n)$ and $\mathbf{C}_{\kappa,j}^{(\ell)}(\mathbf{y}_n)$, that are used in the Gaussian approximation $\tilde{\kappa}_{n,j}^{(\ell)}(\mathbf{y}_n;\mathbf{z}_j) = \mathcal{N}\big(\mathbf{z}_j;\boldsymbol{\mu}_{\kappa,j}^{(\ell)}(\mathbf{y}_n),\mathbf{C}_{\kappa,j}^{(\ell)}(\mathbf{y}_n)\big)$ as discussed in Section III-C. This derivation relies on an interpretation of $\kappa_{n,j}^{(\ell)}(\mathbf{y}_n;\mathbf{z}_j)$ as a probability density function (PDF) of $\mathbf{z}_{k,j}$ conditioned on $\mathbf{y}_n$ and an interpretation of $\beta_{n,j}^{(\ell)}(\mathbf{y}_n)$ as a PDF of $\mathbf{y}_n$. Consequently, we introduce the notation $\tilde{p}^{(\ell)}(\mathbf{z}_j|\mathbf{y}_n) \triangleq \kappa_{n,j}^{(\ell)}(\mathbf{y}_n;\mathbf{z}_j)$ and $\tilde{p}_j^{(\ell)}(\mathbf{y}_n) \triangleq \beta_{n,j}^{(\ell)}(\mathbf{y}_n)$. Based on this new notation, the expression for $\kappa_{n,j}^{(\ell)}(\mathbf{y}_n;\mathbf{z}_j)$ in [1, Eq. (5)], reads

$$\tilde{p}^{(\ell)}(\mathbf{z}_j|\mathbf{y}_n) = \sum_{\mathbf{y}\setminus\mathbf{y}_n} p(\mathbf{z}_j|\mathbf{y}) \prod_{\substack{n'=1\\n'\neq n}}^{N} \tilde{p}_j^{(\ell)}(\mathbf{y}_{n'}). \tag{1}$$

1.1 Derivation of the Mean Vector $\boldsymbol{\mu}_{\kappa,j}^{(\ell)}(\mathbf{y}_n)$

The mean $\boldsymbol{\mu}_{\kappa,j}^{(\ell)}(\mathbf{y}_n)$, can now be computed as the expectation of $\mathbf{z}_j$ with respect to $\tilde{p}^{(\ell)}(\mathbf{z}_j|\mathbf{y}_n)$, i.e.,

$$\begin{aligned}
\boldsymbol{\mu}_{\kappa,j}^{(\ell)}(\mathbf{y}_n) &= \int \mathbf{z}_j \Bigg(\sum_{\mathbf{y}\setminus\mathbf{y}_n} p(\mathbf{z}_j|\mathbf{y}) \prod_{\substack{\tilde{n}=1\\\tilde{n}\neq n}}^{N} \tilde{p}_j^{(\ell)}(\mathbf{y}_{\tilde{n}}) \Bigg) \,\mathrm{d}\mathbf{z}_j \\
&= \sum_{\mathbf{y}\setminus\mathbf{y}_n} \Bigg(\int \mathbf{z}_j p(\mathbf{z}_j|\mathbf{y}) \,\mathrm{d}\mathbf{z}_j \Bigg) \prod_{\substack{\tilde{n}=1\\\tilde{n}\neq n}}^{N} \tilde{p}_j^{(\ell)}(\mathbf{y}_{\tilde{n}}) \\
&= \sum_{\mathbf{y}\setminus\mathbf{y}_n} \mathrm{E}(\mathbf{z}_j|\mathbf{y}) \prod_{\substack{\tilde{n}=1\\\tilde{n}\neq n}}^{N} \tilde{p}_j^{(\ell)}(\mathbf{y}_{\tilde{n}}).
\end{aligned} \tag{2}$$

By further using the measurement model in [1, Eq. (1)], we obtain

$$\begin{aligned}\boldsymbol{\mu}_{\kappa,j}^{(\ell)}(\mathbf{y}_n) &= \sum_{\mathbf{y}\setminus\mathbf{y}_n} \mathrm{E}\Big(\sum_{n'=1}^{N} r_{n'}\mathbf{h}_{j,n'} + \boldsymbol{\epsilon}_j \mid \mathbf{y} \Big) \prod_{\substack{\tilde{n}=1 \\ \tilde{n}\neq n}}^{N} \tilde{p}_j^{(\ell)}(\mathbf{y}_{\tilde{n}}) \\ &= \sum_{\mathbf{y}\setminus\mathbf{y}_n} \Big(\sum_{n'=1}^{N} r_{n'}\boldsymbol{\mu}_j(\mathbf{x}_{n'}) \Big) \prod_{\substack{\tilde{n}=1 \\ \tilde{n}\neq n}}^{N} \tilde{p}_j^{(\ell)}(\mathbf{y}_{\tilde{n}}) \\ &= \sum_{n'=1}^{N} \sum_{\mathbf{y}\setminus\mathbf{y}_n} r_{n'}\boldsymbol{\mu}_j(\mathbf{x}_{n'}) \prod_{\substack{\tilde{n}=1 \\ \tilde{n}\neq n}}^{N} \tilde{p}_j^{(\ell)}(\mathbf{y}_{\tilde{n}}) \end{aligned} \tag{3}$$

where $\boldsymbol{\mu}_j(\mathbf{x}_n)$ is the mean of the Gaussian PDF $p(\mathbf{h}_{j,n}|\mathbf{x}_n)$ introduced in Section II-A.

Since $\tilde{p}_j^{(\ell)}(\mathbf{y}_{\tilde{n}})$ are PDFs that sum and integrate to one, we obtain

$$\sum_{\mathbf{y}\setminus\mathbf{y}_n} r_{n'}\boldsymbol{\mu}_j(\mathbf{x}_{n'}) \prod_{\substack{\tilde{n}=1 \\ \tilde{n}\neq n}}^{N} \tilde{p}_j^{(\ell)}(\mathbf{y}_{\tilde{n}}) = \sum_{\mathbf{y}_{n'}} r_{n'}\boldsymbol{\mu}_j(\mathbf{x}_{n'})\tilde{p}_j^{(\ell)}(\mathbf{y}_{n'})$$

for $n' \neq n$, and

$$\sum_{\mathbf{y}\setminus\mathbf{y}_n} r_{n'}\boldsymbol{\mu}_j(\mathbf{x}_{n'}) \prod_{\substack{\tilde{n}=1 \\ \tilde{n}\neq n}}^{N} \tilde{p}_j^{(\ell)}(\mathbf{y}_{\tilde{n}}) = r_n\boldsymbol{\mu}_j(\mathbf{x}_n).$$

for $n' = n$. By plugging this result into (3), we can write

$$\begin{aligned}\boldsymbol{\mu}_{\kappa,j}^{(\ell)}(\mathbf{y}_n) &= r_n\boldsymbol{\mu}_j(\mathbf{x}_n) + \sum_{\substack{n'=1 \\ n'\neq n}}^{N} \sum_{\mathbf{y}_{n'}} r_{n'}\boldsymbol{\mu}_j(\mathbf{x}_{n'})\tilde{p}_j^{(\ell)}(\mathbf{y}_{n'}) \\ &= r_n\boldsymbol{\mu}_j(\mathbf{x}_n) + \sum_{\substack{n'=1 \\ n'\neq n}}^{N} \sum_{r_{n'}\in\{0,1\}} \int r_{n'}\boldsymbol{\mu}_j(\mathbf{x}_{n'})\tilde{p}_j^{(\ell)}(\mathbf{x}_{n'}, r_{n'})\, \mathrm{d}\mathbf{x}_{n'} \\ &= r_n\boldsymbol{\mu}_j(\mathbf{x}_n) + \sum_{\substack{n'=1 \\ n'\neq n}}^{N} \int \boldsymbol{\mu}_j(\mathbf{x}_{n'})\tilde{p}_j^{(\ell)}(\mathbf{x}_{n'}, 1)\, \mathrm{d}\mathbf{x}_{n'}. \end{aligned} \tag{4}$$

Finally, we introduce $\boldsymbol{\mu}_{n,j}^{(\ell)} = \int \boldsymbol{\mu}_j(\mathbf{x}_n)\tilde{p}_j^{(\ell)}(\mathbf{x}_n, 1)\, \mathrm{d}\mathbf{x}_n$ to get the expression

$$\boldsymbol{\mu}_{\kappa,j}^{(\ell)}(\mathbf{y}_n) = r_n\boldsymbol{\mu}_j(\mathbf{x}_n) + \sum_{\substack{n'=1 \\ n'\neq n}}^{N} \boldsymbol{\mu}_{n',j}^{(\ell)}. \tag{5}$$

1.2 Derivation of the Covariance Matrix $\mathbf{C}_{\kappa,j}^{(\ell)}(\mathbf{y}_n)$

To get the covariance $\mathbf{C}_{\kappa,j}^{(\ell)}(\mathbf{y}_n)$, we first compute the correlation matrix $\mathbf{R}_{\kappa,j}^{(\ell)}(\mathbf{y}_n)$, as the expectation of $\mathbf{z}_j\mathbf{z}_j^{\mathrm{T}}$ with respect to $\tilde{p}^{(\ell)}(\mathbf{z}_j|\mathbf{y}_n)$

$$\begin{aligned}\mathbf{R}_{\kappa,j}^{(\ell)}(\mathbf{y}_n) &= \int \mathbf{z}_j\mathbf{z}_j^{\mathrm{T}}\Big(\sum_{\mathbf{y}\setminus\mathbf{y}_n} p(\mathbf{z}_j|\mathbf{y}) \prod_{\substack{\tilde{n}=1\\ \tilde{n}\neq n}}^{N} \tilde{p}_j^{(\ell)}(\mathbf{y}_{\tilde{n}})\Big)\,\mathrm{d}\mathbf{z}_j \\ &= \sum_{\mathbf{y}\setminus\mathbf{y}_n}\Big(\int \mathbf{z}_j\mathbf{z}_j^{\mathrm{T}} p(\mathbf{z}_j|\mathbf{y})\,\mathrm{d}\mathbf{z}_j\Big) \prod_{\substack{\tilde{n}=1\\ \tilde{n}\neq n}}^{N} \tilde{p}_j^{(\ell)}(\mathbf{y}_{\tilde{n}}) \\ &= \sum_{\mathbf{y}\setminus\mathbf{y}_n} \mathrm{E}(\mathbf{z}_j\mathbf{z}_j^{\mathrm{T}}|\mathbf{y}) \prod_{\substack{\tilde{n}=1\\ \tilde{n}\neq n}}^{N} \tilde{p}_j^{(\ell)}(\mathbf{y}_{\tilde{n}}). \end{aligned} \tag{6}$$

Since r_n is binary, we have $r_n^2 = r_n$. In addition, $\mathrm{E}(\mathbf{h}_{j,n}\mathbf{h}_{j,n}^{\mathrm{T}}|\mathbf{x}) = \mathbf{C}_j(\mathbf{x}_n) + \boldsymbol{\mu}_j(\mathbf{x}_n)\boldsymbol{\mu}_j^{\mathrm{T}}(\mathbf{x}_n)$, where $\mathbf{C}_j(\mathbf{x}_n)$ is the covariance matrix of the Gaussian PDF $p(\mathbf{h}_{j,n}|\mathbf{x}_n)$ introduced in Section II-A. Next, by making use of the measurement model [1, Eq. (5)], we obtain

$$\begin{aligned}\mathbf{R}_{\kappa,j}^{(\ell)}(\mathbf{y}_n) &= \sum_{\mathbf{y}\setminus\mathbf{y}_n} \mathrm{E}\Big(\Big(\sum_{n'=1}^{N} r_{n'}\mathbf{h}_{j,n'} + \boldsymbol{\epsilon}_j\Big)\Big(\sum_{n'=1}^{N} r_{n'}\mathbf{h}_{j,n'} + \boldsymbol{\epsilon}_j\Big)^{\mathrm{T}} \mid \mathbf{y}\Big) \prod_{\substack{\tilde{n}=1\\ \tilde{n}\neq n}}^{N} \tilde{p}_j^{(\ell)}(\mathbf{y}_{\tilde{n}}) \\ &= \sum_{\mathbf{y}\setminus\mathbf{y}_n}\Bigg(\sum_{n'=1}^{N} r_{n'}\big(\mathbf{C}_j(\mathbf{x}_{n'}) + \boldsymbol{\mu}_j(\mathbf{x}_{n'})\boldsymbol{\mu}_j^{\mathrm{T}}(\mathbf{x}_{n'})\big) + \mathbf{C}_{\boldsymbol{\epsilon}} \\ &\qquad + \sum_{n'=1}^{N}\sum_{\substack{n''=1\\ n''\neq n'}}^{N} r_{n'}r_{n''}\boldsymbol{\mu}_j(\mathbf{x}_{n'})\boldsymbol{\mu}_j^{\mathrm{T}}(\mathbf{x}_{n''})\Bigg) \prod_{\substack{\tilde{n}=1\\ \tilde{n}\neq n}}^{N} \tilde{p}_j^{(\ell)}(\mathbf{y}_{\tilde{n}}) \\ &= \mathbf{C}_{\boldsymbol{\epsilon}} + \sum_{n'=1}^{N} \underbrace{\sum_{\mathbf{y}\setminus\mathbf{y}_n} r_{n'}\big(\mathbf{C}_j(\mathbf{x}_{n'}) + \boldsymbol{\mu}_j(\mathbf{x}_{n'})\boldsymbol{\mu}_j^{\mathrm{T}}(\mathbf{x}_{n'})\big) \prod_{\substack{\tilde{n}=1\\ \tilde{n}\neq n}}^{N} \tilde{p}_j^{(\ell)}(\mathbf{y}_{\tilde{n}})}_{\triangleq\mathbf{R}_1} \\ &\quad + \sum_{n'=1}^{N}\sum_{\substack{n''=1\\ n''\neq n'}}^{N} \underbrace{\sum_{\mathbf{y}\setminus\mathbf{y}_n} r_{n'}r_{n''}\boldsymbol{\mu}_j(\mathbf{x}_{n'})\boldsymbol{\mu}_j^{\mathrm{T}}(\mathbf{x}_{n''}) \prod_{\substack{\tilde{n}=1\\ \tilde{n}\neq n}}^{N} \tilde{p}_j^{(\ell)}(\mathbf{y}_{\tilde{n}})}_{\triangleq\mathbf{R}_2}. \end{aligned} \tag{7}$$

Next, we discuss the detailed expression of $\mathbf{R}_1$ and $\mathbf{R}_2$. For $\mathbf{R}_1$, we obtain

$$\mathbf{R}_1 = r_{n'}\big(\mathbf{C}_j(\mathbf{x}_{n'}) + \boldsymbol{\mu}_j(\mathbf{x}_{n'})\boldsymbol{\mu}_j^{\mathrm{T}}(\mathbf{x}_{n'})\big)$$

for $n' = n$, and

$$\mathbf{R}_1 = \sum_{\mathbf{y}_{n'}} r_{n'}\big(\mathbf{C}_j(\mathbf{x}_{n'}) + \boldsymbol{\mu}_j(\mathbf{x}_{n'})\boldsymbol{\mu}_j^{\mathrm{T}}(\mathbf{x}_{n'})\big)\tilde{p}_j^{(\ell)}(\mathbf{y}_{n'})$$

otherwise. Similarly, for $\mathbf{R}_2$, we get

$$\mathbf{R}_2 = r_n\boldsymbol{\mu}_j(\mathbf{x}_n)\sum_{\mathbf{y}_{n'}} r_{n'}\boldsymbol{\mu}_j^{\mathrm{T}}(\mathbf{x}_{n'})\tilde{p}_j^{(\ell)}(\mathbf{y}_{n'})$$

if $n' = n$ or $n'' = n$, and

$$\mathbf{R}_2 = \Big(\sum_{\mathbf{y}_{n'}} r_{n'} \boldsymbol{\mu}_j(\mathbf{x}_{n'}) \tilde{p}_j^{(\ell)}(\mathbf{y}_{n'}) \Big) \Big(\sum_{\mathbf{y}_{n''}} r_{n''} \boldsymbol{\mu}_j(\mathbf{x}_{n''}) \tilde{p}_j^{(\ell)}(\mathbf{y}_{n''}) \Big)^{\mathrm{T}}$$

otherwise. By using Using these results in (7), we obtain

$$\begin{aligned}
\mathbf{R}_{\kappa,j}^{(\ell)}(\mathbf{y}_n) &= \mathbf{C}_{\boldsymbol{\epsilon}} + r_n \mathbf{C}_j(\mathbf{x}_n) + r_n \boldsymbol{\mu}_j(\mathbf{x}_n) \boldsymbol{\mu}_j^{\mathrm{T}}(\mathbf{x}_n) \\
&\quad + \sum_{\substack{n'=1 \\ n' \neq n}}^{N} \sum_{\mathbf{y}_{n'}} r_{n'} \Big(\mathbf{C}_j(\mathbf{x}_{n'}) + \boldsymbol{\mu}_j(\mathbf{x}_{n'}) \boldsymbol{\mu}_j^{\mathrm{T}}(\mathbf{x}_{n'}) \Big) \tilde{p}_j^{(\ell)}(\mathbf{y}_{n'}) \\
&\quad + 2 r_n \boldsymbol{\mu}_j(\mathbf{x}_n) \sum_{\substack{n'=1 \\ n' \neq n}}^{N} \sum_{\mathbf{y}_{n'}} r_{n'} \boldsymbol{\mu}_j^{\mathrm{T}}(\mathbf{x}_{n'}) \tilde{p}_j^{(\ell)}(\mathbf{y}_{n'}) \\
&\quad + \sum_{\substack{n'=1 \\ n' \neq n}}^{N} \sum_{\substack{n''=1 \\ n'' \neq n,n'}}^{N} \Big(\sum_{\mathbf{y}_{n'}} r_{n'} \boldsymbol{\mu}_j(\mathbf{x}_{n'}) \tilde{p}_j^{(\ell)}(\mathbf{y}_{n'}) \Big) \Big(\sum_{\mathbf{y}_{k,n''}} r_{n''} \boldsymbol{\mu}_j(\mathbf{x}_{n''}) \tilde{p}_j^{(\ell)}(\mathbf{y}_{n''}) \Big)^{\mathrm{T}} \\
&= \mathbf{C}_{\boldsymbol{\epsilon}} + r_n \mathbf{C}_j(\mathbf{x}_n) + r_n \boldsymbol{\mu}_j(\mathbf{x}_n) \boldsymbol{\mu}_j^{\mathrm{T}}(\mathbf{x}_n) + 2 r_n \boldsymbol{\mu}_j(\mathbf{x}_n) \sum_{\substack{n'=1 \\ n' \neq n}}^{N} \boldsymbol{\mu}_{n',j}^{(\ell)\mathrm{T}} \\
&\quad + \sum_{\substack{n'=1 \\ n' \neq n}}^{N} \mathbf{R}_{n',j}^{(\ell)} + \sum_{\substack{n'=1 \\ n' \neq n}}^{N} \sum_{\substack{n''=1 \\ n'' \neq n,n'}}^{N} \boldsymbol{\mu}_{n',j}^{(\ell)} \boldsymbol{\mu}_{n'',j}^{(\ell)\mathrm{T}}
\end{aligned} \tag{8}$$

where we have introduced

$$\begin{aligned}
\mathbf{R}_{n,j}^{(\ell)} &= \mathrm{E}_{n,j}^{(\ell)} \Big(\mathbf{C}_j(\mathbf{x}_n) + \boldsymbol{\mu}_j(\mathbf{x}_n) \boldsymbol{\mu}_j^{\mathrm{T}}(\mathbf{x}_n) \Big) \\
&= \int \Big(\mathbf{C}_j(\mathbf{x}_n) + \boldsymbol{\mu}_j(\mathbf{x}_n) \boldsymbol{\mu}_j^{\mathrm{T}}(\mathbf{x}_n) \Big) \tilde{p}_j^{(\ell)}(\mathbf{x}_n, 1) \, \mathrm{d}\mathbf{x}_n.
\end{aligned}$$

The final covariance matrix can now be computed as

$$\begin{aligned}
\mathbf{C}_{\kappa,j}^{(\ell)}(\mathbf{y}_n) &= \mathbf{R}_{\kappa,j}^{(\ell)}(\mathbf{y}_n) - \Big(\boldsymbol{\mu}_{\kappa,j}^{(\ell)}(\mathbf{y}_n) \Big) \Big(\boldsymbol{\mu}_{\kappa,j}^{(\ell)}(\mathbf{y}_n) \Big)^{\mathrm{T}} \\
&= r_n \mathbf{C}_j(\mathbf{x}_n) + \mathbf{C}_{\boldsymbol{\epsilon}} + \sum_{\substack{n'=1 \\ n' \neq n}}^{N} \Big(\mathbf{R}_{n',j}^{(\ell)} - \boldsymbol{\mu}_{n',j}^{(\ell)} \boldsymbol{\mu}_{n',j}^{(\ell)\mathrm{T}} \Big).
\end{aligned} \tag{9}$$

1.3 Qualitative Analysis of $\tilde{\kappa}_{n,j}^{(\ell)}(\mathbf{y}_n)$

In this section, we evaluate the impact of the approximation of $\kappa_{n,j}^{(\ell)}(\mathbf{y}_n)$ in a simple toy example with closely objects. In particular, we consider a scenario with only two objects which are located at $\mathbf{p}_1 = [4 \; 4]^{\mathrm{T}}$ and $\mathbf{p}_2 = [5 \; 5]^{\mathrm{T}}$. The two objects are modeled by two potential object (PO) states, i.e., $n \in \{1, 2\}$. It is assumed that the prediction step has been performed and that the message $\alpha_n(\mathbf{x}_n, 1)$, are described by particle representations obtained by sampling from the PDF $\mathcal{N}(\mathbf{p}_n; \boldsymbol{\mu}_n, 0.3\mathbf{I}_2) \delta(\mathbf{v}_n) \delta(\gamma_n - 60)$. Here, $\boldsymbol{\mu}_1 = \mathbf{p}_1$ and $\boldsymbol{\mu}_2 = \mathbf{p}_2$ and $\alpha_n(\mathbf{x}_n, 0) = 0$ for $n \in \{1, 2\}$. The parameters of the measurement model are identical to those in [1, Sec. IV] except that we only consider a 10×10 grid of data cells where each cell is a square of 1m length. The underlying

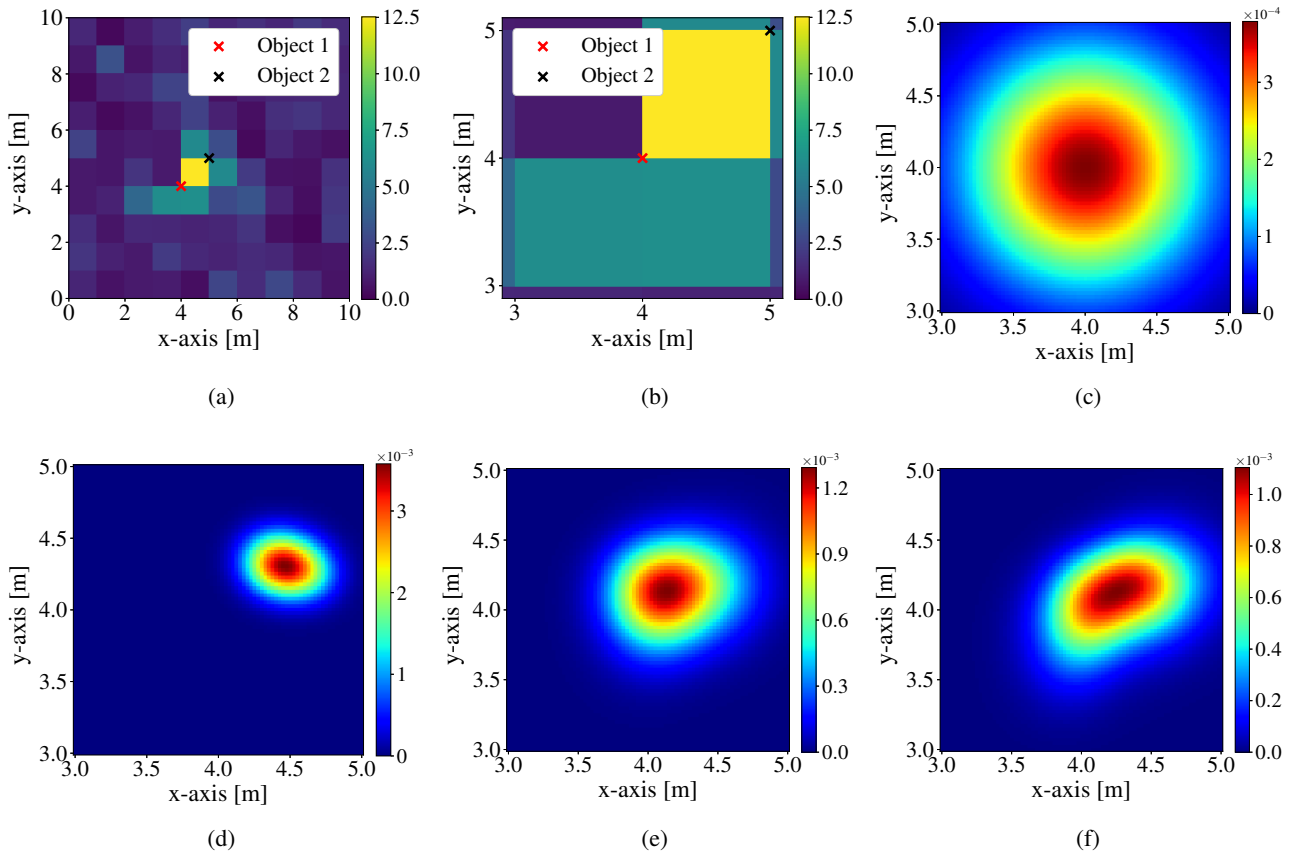

Figure 1: Simple toy example with interacting objects. Measurements with overlayed object positions in different scales are shown in (a) and (b). The positional information of $\alpha_1(\mathbf{x}_1, 1)$ is shown (c). Positional information $\tilde{f}(\mathbf{x}_1, 1)$ provided by TBD-MB, TBD-BP with approximated messages $\tilde{\kappa}_{n,j}^{(\ell)}(\mathbf{y}_n)$, and TBD-BP with exact messages $\kappa_{n,j}^{(\ell)}(\mathbf{y}_n)$ is shown in (d), (e), and (f), respectively.

scenario is shown in Figure 1a and the positional information of $\alpha_1(\mathbf{x}_1, 1)$ in Figure 1c. We here compare the belief of PO state $n = 1$ using (i) TBD-MB, (ii) TBD-BP with approximated messages $\tilde{\kappa}_{1,j}^{(\ell)}(\mathbf{y}_1)$, and (iii) TBD-BP with exact messages $\kappa_{1,j}^{(\ell)}(\mathbf{y}_1)$. The number of message passing iterations for both versions of TBD-BP was set to $L = 1$. The results in Figures 1(c)–(e) show that the beliefs provided by (ii) and (iii) are very similar, whereas the one provided by TBD-MB is quite different. We can thus conclude that for the considered scenario, the proposed approximation for computing $\kappa_{n,j}^{(\ell)}(\mathbf{y}_n)$ is accurate and that TBD-MB provides inaccurate results in the case of closely spaced objects. Note that TBD-BP without approximation of $\kappa_{n,j}^{(\ell)}(\mathbf{y}_n)$ provides the true marginal posterior PDFs.

2 Further Simulation Results

In order to provide more insights into the experiments conducted in Section IV, we show in Figure 2 the object's position, the object's trajectory, and intensity measurements for four different time steps for a single simulation run. Note that there are 50 time steps in total. The figure shows that when objects come in close proximity (cf. Figure (2b) and (2c)), the pixels have higher intensity values due to the contribution from multiple objects. The GOSPA performance for this specific simulation run is shown in Figure 3. It is seen that both TBD-IEMB and the proposed TBD-BP perform significantly better that TBD-MB. The reason is that both TBD-IEMB and TBD-BP systematically model object interaction while TBD-MB does not. We refer here to the averaged GOSPA curves in the main paper (cf. Section IV, Fig. 2), where it can be seen that TBD-BP outperforms TBD-IEMB for all time steps k.

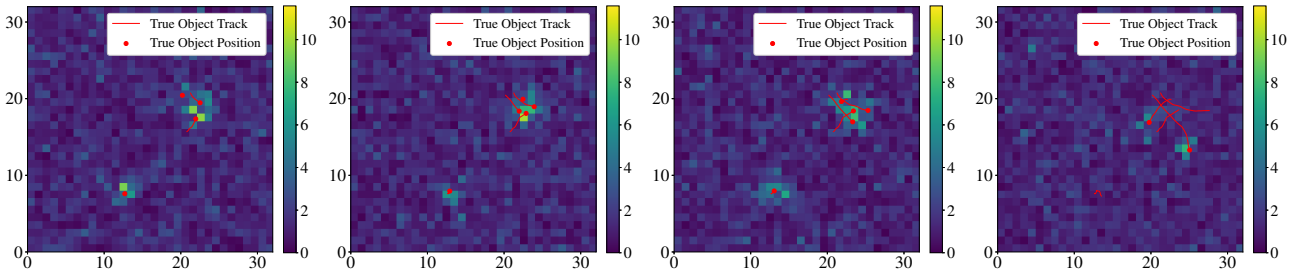

(a) (b) (c) (d)

Figure 2: Object's positions, object's trajectories, and intensity measurements for $\sigma_S^2 = 1$ at time steps (a) $k = 14$, (b) $k = 21$, (c) $k = 27$, and (d) $k = 43$.

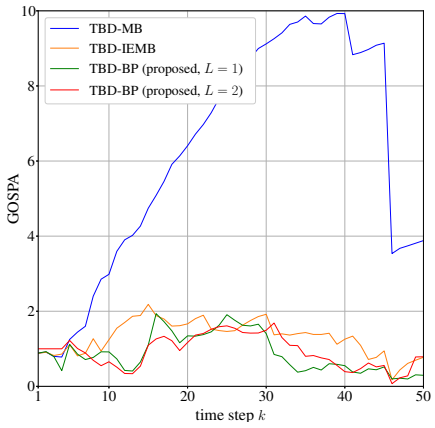

(a)

Figure 3: GOSPA error of a single simulation run for TBD-MB, TBD-IEMB, and TBD-BP.

3 Complexity Analysis

In this section, we provide a quantitative complexity analysis of our proposed TBD-BP method. In particular, we measure the runtime of TBD-BP for a varying number of objects. The simulation scenario and filter settings are equal to those described in [1, Sec. IV] with the only difference that the objects exist for all 50 time steps as long as they do not leave the region of interest (ROI). Runtime averaged over all 50 time steps and 400 simulation runs are shown in Figure 4. The runtimes show a linear increase with the number of objects and thus confirm the linear scaling of the computational complexity derived in [1, Sec. III-C].

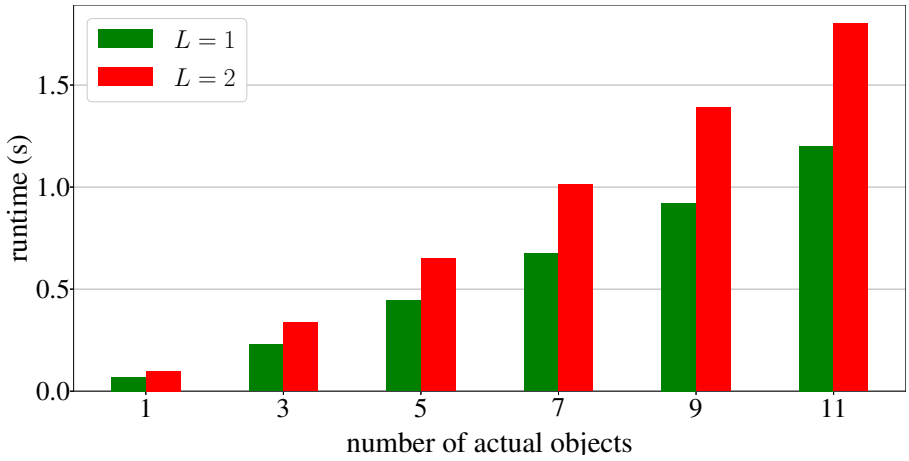

Figure 4: Average filter runtimes for a different number of objects and message passing iterations ($L = 1$ and $L = 2$).

References

[1] M. Liang, T. Kropfreiter, and F. Meyer, "A BP method for track-before-detect," *IEEE Signal Process. Lett.*, 2023, to appear.